



## DESIGN, SIMULATION AND ANALYSIS OF AN INTELLIGENT LEAD-ACID BATTERY CHARGER FED BY SOLAR SYSTEM

\*Hussain S. Maraud<sup>1</sup>, Dr. Isam M. Abdulbaqi<sup>2</sup>, Ammar I. Majeed<sup>3</sup>

- 1) Engineer, Electrical Engineering Department, Al-Mustansiriayah University, Baghdad, Iraq.
- 2) Prof., Electrical Engineering Department, Al-Mustansiriayah University, Baghdad, Iraq.
- 3) Lecturer, Electrical Engineering Department, Al-Mustansiriayah University, Baghdad, Iraq.

**Abstract:** The objectives of this work are to design, simulate and analyze the operation of an intelligent lead-acid battery charger supplied from a two (250W) nominal power, Photovoltaic (PV) panel in parallel to charge two (200Ah) capacity lead-acid batteries in parallel. The storage battery's effectiveness depends on the charging process. Hence, this research deals with the study, simulation and design of an intelligent charger fed by solar system due to the latest technologies. The developed charging method entitled "the decreased charging current based on SOC" is adopted in this research to charge a lead-acid battery. The principle of decreased charging current is to make the real charging current as close as possible to the maximum acceptable current. The advantage of this technique is to mix between the rapidity of charging and prevents of the overcharging and generates gases. Also, the design considers different operating conditions of load, battery state of charge (SOC) and ambient effect in order to achieve the best charging condition of the batteries and to be compatible with the user requirements. Therefore, this technique of charging can be considered as intelligent charging compared to traditional charging ways, which are often either an a constant charging current or a constant charging voltage. The flexible, simple and cheap design is the objective of this research. The obtained results agree with the research objective.

**Keywords:** Lead-Acid Battery, SOC, Intelligent Charger.

### تصميم ومحاكاة وتحليل الشاحنة الذكية لبطارية الحمض الرصاصية المغذاة من منظومة الطاقة الشمسية

**الخلاصة:** تعتبر الشاحنة من أهم أجزاء المنظومة الشمسية وذلك لكون بطاريات الخزن هي الجزء الوحيد المحدود العمر منها. إن فعالية هذه البطاريات تعتمد على عملية الشحن، عليه يهتم هذا البحث بدراسة و تمثيل و تصميم شاحنة ذكية تتغذى من منظومة شمسية باستخدام أحدث التقنيات. سُميت هذه الشاحنة بالذكية اعتمادا على تقنية الشحن المقترحة. حيث تم اعتماد تقنية الشحن الموسومة (تخفيض تيار الشحن اعتمادا على حالة الشحنة في البطارية (SOC)) في هذا البحث لشحن بطارية الرصاص الحمضية. إن مبدأ هذه التقنية هو جعل تيار الشحن الفعلي أقربا يمكن من الحد الأقصى من تيار الشحن المقبول. إن فائدة هذه التقنية هي الدمج بين سرعة الشحن ومنع حالة الإفراط في الشحن وتولد الغازات. لذا تعتبر هذه التقنية من الشحن ذكية مقارنة بالطرق التقليدية للشحن، والتي غالبا ما تكون أما بتيار ثابت أو فولتية ثابتة. إن التصميم أخذ بالاعتبار حالات تحميل و حالات شحنة بطارية و تأثيرات بيئية مختلفة و أن تكون مناسبة لمتطلبات المستخدم للمنظومة. إن الغاية من البحث هو تصميم شاحنة مرنة و بسيطة و رخيصة. إن النتائج المتحصلة جاءت متوافقة مع أهداف البحث.

\*Corresponding Author [hussainalkuraeshy@yahoo.com](mailto:hussainalkuraeshy@yahoo.com)

## 1. Introduction

The charger is the most important part of the solar system because the only limited-age part of this system is the storage batteries. So, the charger design must take into consideration the latest knowledge in this field such that it must be efficient, reliable, flexible, simple and cheap. The simulation depends on software (Proteus) computer package to study the response of system. The maximum power point tracking (MPPT) technique adopted to achieve as maximum as possible energy from the panel. This power used for charging the battery and feeding the load at the same time with a priority decided by the user, depending on the battery condition monitored by the charger and on the load condition and requirements.

Because the battery must be replaced periodically so it increase the cost of the solar system, hence, the charger must be well designed to keep the battery healthy life as long as possible. For this purpose, the Lead-acid battery transient and steady state conditions are considered in its equivalent circuit adopted in the simulation. The battery equivalent circuit accomplishes the chemical and electrical behavior during charging and discharging conditions.

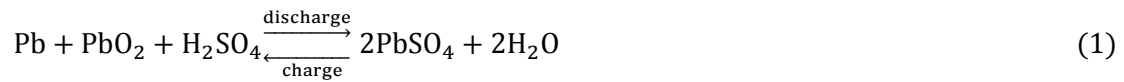
The Programmable Interface Controller (PIC) used to perform the matching process between the panel and the load to keep it work at MPP, and to control the charging current avoiding the battery gassing voltage and heating due to overcharging during the charging process.

The majorities of the research which dealt with this subject and that have been mentioned in the list of references adopt the charge of batteries with constant current or constant voltage and does not regard SOC of batteries thought the charging process to excellently prevent the dangers of overcharging and deep discharge and prolong the battery life-time. Also, these researches doesn't match between excerpt the maximum PV power and best charging techniques and don't considers different operating conditions of load. Hence, this thesis deals with the study, simulation and design of an intelligent charger fed by solar system due to the latest technologies. The design considers different operating conditions of load, battery state of charge and ambient effect in order to achieve the best charging condition of the batteries and to be compatible with the user requirements.

## 2. Lead-Acid Battery

### 2.1. Lead-acid Battery Chemical Theory

The cell of a lead-acid battery comprises a set of positive and negative electrodes. In full charge state, the positive electrode is lead dioxide ( $\text{PbO}_2$ ) and the negative electrode is the sponge lead (Pb) and the electrolyte solution is the sulfuric acid ( $\text{H}_2\text{SO}_4$ ) [1] [2]. For charging and discharging process, the chemical reaction could convert the energy from electrical into chemical and back again. The following equation shows the process of a chemical reaction inside the battery during charging and discharging [1]:



The nominal potential of each Pb/PbO<sub>2</sub> cell is about 2V. So, in order to prevent the overcharging and gassing problems, the cell is charged for less than 2.4V which is known the gassing voltage. The cell charging and discharging terminal voltage characteristic is shown in Fig. 1[3].

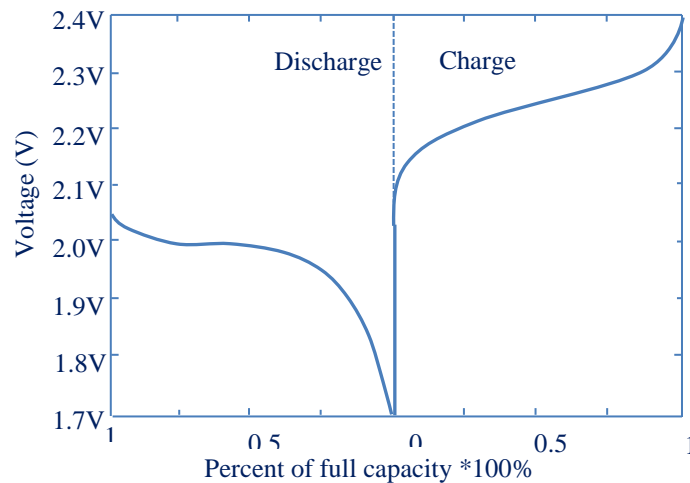


Figure 1. Discharge and charge voltage of a lead-acid battery cell [3]

## 2.2. State of Charge (SOC)

State of charge (SOC) and depth of charge (DOC) are variables that can describe the battery charge. The main difference is that the SOC describes the percentage of remaining charge relative to the nominal capacity of battery while the DOC represents that relative to the actual capacity under a specific discharge current.

These two variables can be achieved by calculating the charge consumed and the battery capacity [2]:

$$\text{SOC} = 1 - Q_e/C_{10} \quad (2)$$

$$\text{DOC} = 1 - Q_e/C_I \quad (3)$$

Knowing the State of Charge (SOC) is very important in the charging process of a lead-acid batteries, because it determines the value of instantaneous charging current to prevent the overcharging and gassing problems. Where as the SOC is increased during the charging process and the battery is near from fully charging condition, the charging current must be decreased gradually to overcome the gassing and electrolyte losses and to increase the useful service life for the battery [2].

## 2.3. Effect of Specific Gravity on the Battery State of Charge

Specific Gravity (SG) is a measurement of concentration of electrolyte solution. SG represents the ratio of solution to the water density. The specific gravity of electrolyte is

related to the state of charge (remain of full capacity) of a lead-acid battery. Where as the battery is charging, the sulfuric acid will be produced and SG is increasing, whereas the opposite will happen during the discharge. For full charge capacity of a lead-acid battery, SG of electrolyte is in the range of 1.25 (kg/L) to 1.28 (kg/L) at 27°C. Therefore, the SG is considered as one of the methods to calculate the state of charge of lead-acid batteries.

#### 2.4. Electromotive Force of a Lead-Acid Battery

The electromotive force or the open circuit voltage of a lead-acid battery cell can be obtained by using the Nernst's equation. This equation written as [1] [3]:

$$\text{EMF} = 2.01 + 0.0296 \ln \frac{\alpha^2(\text{H}_2\text{SO}_4)}{\alpha^2(\text{H}_2\text{O})} \quad (4)$$

Because the concentration or specific gravity of the electrolyte solution varies through the charging and discharging of the lead-acid battery, the relative activity of  $\text{H}_2\text{SO}_4$  will also be changed in the Nernst's equation. Due to this, the open circuit voltage of a lead-acid battery is changed proportionally with respect to temperature and specific gravity of electrolyte solution. Therefore, by knowing the open circuit voltage of lead-acid battery and temperature, specific gravity of electrolyte solution can be determined and thus determine the state of charge. Graph in Fig. 2 shows the relation between the electrolyte specific gravity and the open circuit voltage of a lead-acid battery cell at 25°C [1] & [3].

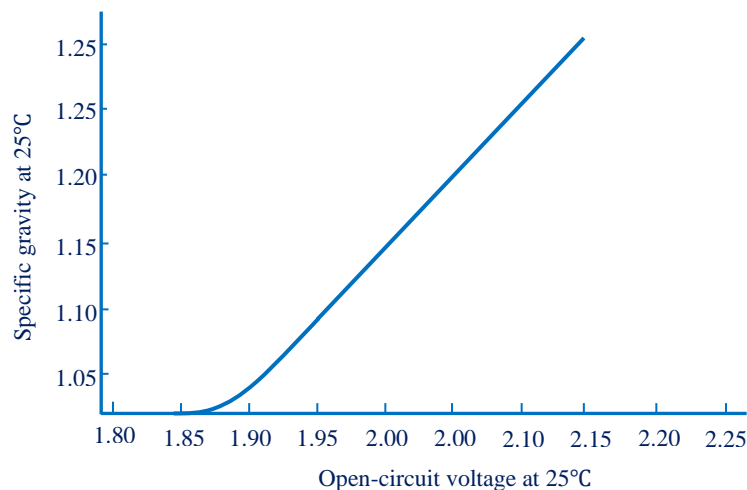


Figure 2. Open-circuit voltage of lead-acid cell as a function of electrolyte specific gravity at 25°C [1]

### 3. Decreased Charging Current Method Based on SOC

The aim of the decreased charging current method is to make the actual charging current closest to the maximum possible current as shown in Fig. 3[4] [5].

It is observed that the maximum charging voltage or overcharging voltage set to  $V_g$  is about 2.4 V/cell. The execution process of this charging method is described as follows: initially charging the batteries with the greatest charge rate  $C_a$ , then the alteration into

$C_{a+1}$  by multiplying it by reduction coefficient ( $\beta = C_n / C_{n-1}$ ) every time the battery voltage arrives to  $V_g$ . Then, the charging rate changes to  $C_{a+2} \dots C_n$  in role. This process is repeatedly continued till the maximum charging current is reached to  $C/100$ . Then a battery charging voltage rise higher than  $2.4V/\text{cell}$  refers a 100% state of charge is reached. In that situation, the charging current has stayed to at least value known as  $I_{\text{trickle}}$  to the indemnity of the controlling unit power, depreciation and the self-discharge of the battery. The first value of the maximum charging current of the battery is renovated when a battery reach to the discharging condition.

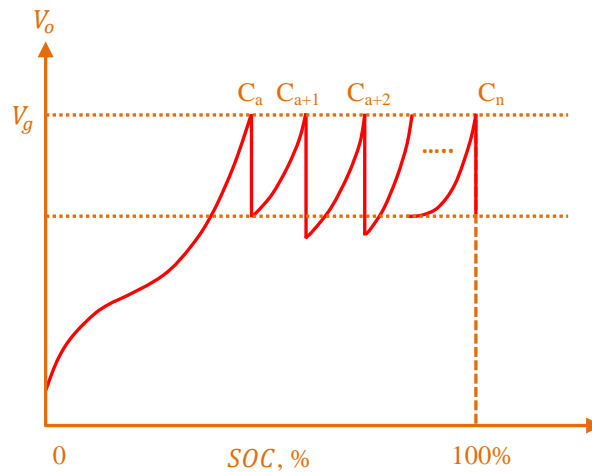


Figure 3. Principle of decreased charging current ( $V_o$  is the battery voltage,  $C_a, C_{a+1}, C_{a+2}, \dots, C_n$ , are charging rates in  $a, a+1, a+2 \dots n$  hour;  $V_g$  is the gassing voltage) [5]

For low panel output power, MPPT algorithm is done, maximizing the power converted to the battery. In respect of other states, the battery charging current is controlled to the maximum acceptable current.

Advantages of the proposed method over traditional charging methods are: The method comparatively makes the batteries reach full capacity in a short time without accurately gauging batteries current; also it reduces the current sensor accuracy required and the cost for circuitry. Furthermore, in contrast to voltage-regulation methods, as the proposed method is based on battery current regulation, it results in a uniform charging of all cells. Thus, it can be effectively used in large battery strings. For these reasons, this method increased battery lifetime by restoring the maximum possible battery (SOC) in the shortest charging time.

The main drawback of this method is that the reduction coefficient  $\beta$  chosen too high or low could result to batteries overcharge or not enough charge, which will adversely affect battery life [4] [5].

## 4. Design and Simulation of an Intelligent Lead-Acid Battery Charger System

### 4.1. Design of Charger Power Circuit

The step-down (Buck) DC-DC converter interfaces between the PV panel and the lead-acid battery to adjust the battery charging current. The diagram of the buck converter is shown in Fig. 4.

The design equations of the buck converter are presented from (5) to (8) [6].

$$V_O = D V_S \quad (5)$$

The inductance and capacitance of buck converter filter are designed based on the following equations to operate the converter in Continuous Current Mode (CCM).

$$C_{\min} = \frac{V_O(1 - D)}{8 \Delta V_O L f_S^2} \quad (6)$$

$$L_{\min} = \frac{V_S}{8 f_S I_{O,\min}} \quad (7)$$

$$I_{O,\min} \geq I_{LB,\max} \quad (8)$$

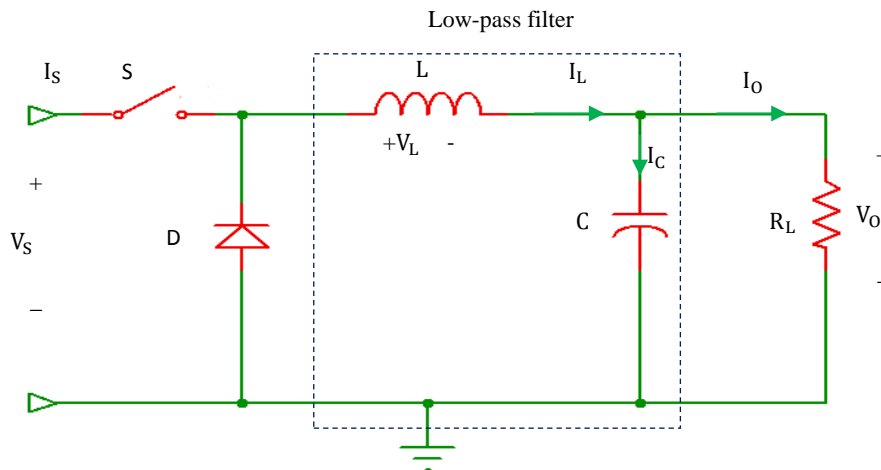


Figure 4. Schematic diagram of buck converter [6]

In this search, the chosen operating switching frequency ( $f_s$ ) of the buck converter that is design in this search is 50 kHz. Also, the step down converter will be operated in CCM as long as the charging current within the range between the greatest charging current (in this search, its take as  $C/12 = 200/12 \cong 16A$ ) ( $C$  is the nominal battery capacity in ampere-hours) to value close to the trickle current (about  $C/40 = 5A$ ). When the charging current less than this value ( $C/40$ ), the inductance current will become discontinues. According to this and by applying equations (5)-(8), the determined values of inductance and capacitance of buck converter filter are  $15\mu H$  and  $4.9 mF$  respectively.

#### 4.2. Modeling and Simulation of Battery

The equivalent circuit of a lead-acid battery is based on nonlinear equations. The equivalent circuit consisted of two main parts: a main branch which approximated the battery dynamics under most conditions, and a parasitic branch which accounted for the

battery behavior at the end of the charging period. The equivalent circuit of the battery is shown in Fig. 5 [7] & [8].

The values of  $E_m, R_0, R_1, C_1, R_2$  and  $I_p$  are determined from (9)-(14) with the given parameters.

$$E_m = E_{m0} - K_E(273 + \theta)(1 - SOC) \tag{9}$$

$$R_0 = R_{00}[1 + A_0(1 - SOC)] \tag{10}$$

$$R_1 = -R_{10}\ln(DOC) \tag{11}$$

$$C_1 = \tau/R_1 \tag{12}$$

$$R_2 = R_{20} \frac{e^{[A_{21}(1-SOC)]}}{1 + e^{(A_{22} I_m/I^*)}} \tag{13}$$

$$I_p = V_{PN}G_{P0} \exp.\left(\frac{V_{PN}}{V_{P0}} + A_P\left(1 - \frac{\theta}{\theta_f}\right)\right) \tag{14}$$

Where:  $A_0, A_{21}, A_{22}, A_P, G_{P0}$  and  $V_{p0}$  are constants for a lead-acid battery.  $R_{00}, R_{10}$  and  $R_{20}$  are parameters related to the state of health (SOH) of battery and they do vary a little among different batteries built with the same technology.

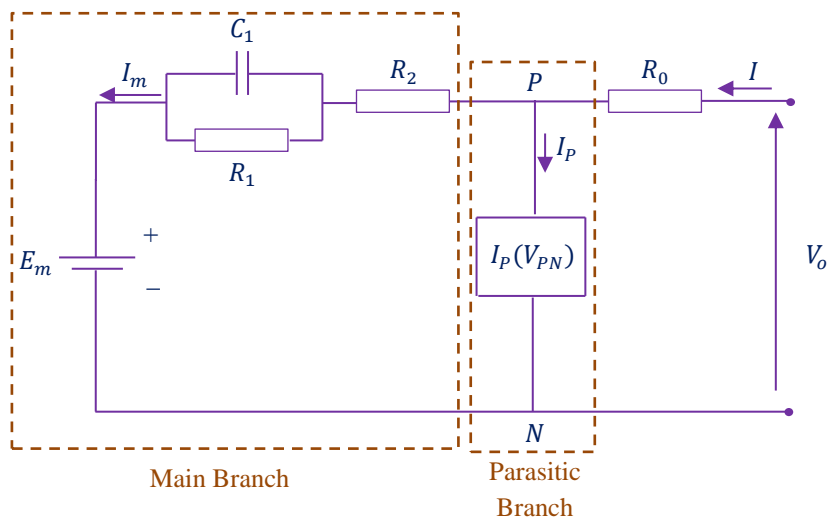


Figure 5. Equivalent circuit of the lead-acid battery [8]

The values of this battery model parameters and constants are reported in the Table 1 for the lead acid battery,  $C_{10}=500$  Ah capacity [7].

Table 1. Parameters of the Lead-Acid Battery model, C10=500 Ah Capacity [7].

Parameter	Value	Parameter	Value	Parameter	Value
$E_{mo}$	2.18 V	$A_{22}$	-8.45	$R_{20}$	15 m $\Omega$
$K_E$	$0.84 \times 10^{-3} \text{V}/^\circ\text{C}$	$\tau$	7200 s	$A_0$	-0.20
$R_{00}$	2.0 m $\Omega$	$G_{P0}$	2 PS	$A_{21}$	-8.0
$R_{10}$	0.4 m $\Omega$	$A_P$	2.0	$\theta_f$	-40 $^\circ\text{C}$

## 5. System Description

The block diagram of the proposed PV battery charging system is shown in Fig. 6. This PV system consists of eight major parts: (1) solar panels, (2) buck converter circuit as the charger power circuit, (3) Voltage and current sensors of panel and battery, which achieved by means of a voltage divider and a Hall-effect current sensors respectively, (4) PIC18F45K22 microcontroller to control the power MOSFET switching duty cycle on the buck converter, (5) gate drive circuit, (6) rechargeable lead-acid battery, (7) resistive load and (8) Liquid Crystal Display (LCD), which informs the user about various parameters of the system operation, for example, it shows the value of charge current.

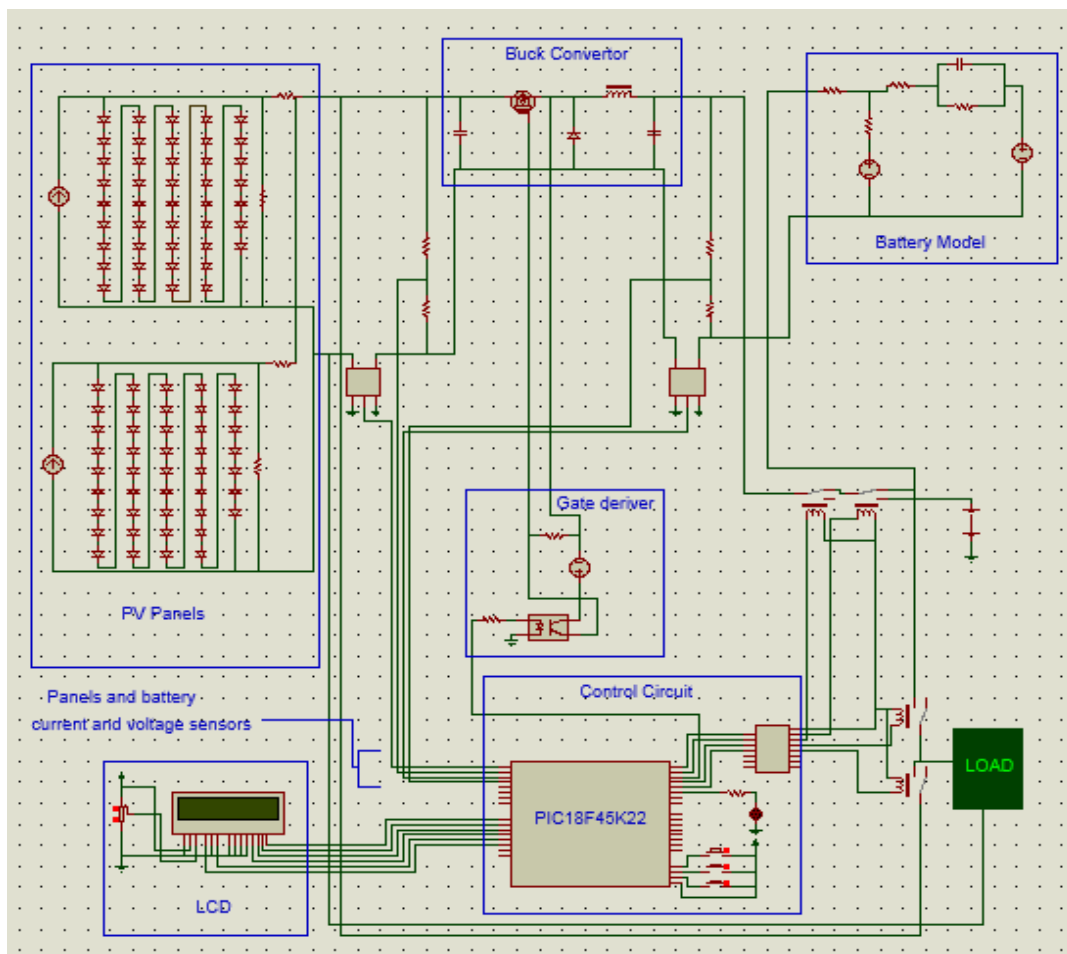


Figure 6. Schematic diagram of the proposed PV battery charger system



The charging algorithm flowchart is shown in Fig. 7. A set of variables is used to store the following parameters of the system operation:

- The minimum and maximum permissible battery voltage and current levels.
- The MPPT control action (variable B in Fig. 7, taking values 1 or 0), indicating whether the MPPT process must be performed or the charging current must be decreased (if  $B=1$  then MPPT is performed; except that, the charging current must be decreased where, in this case, it is higher than the maximum battery current). The maximum battery charging current is set to  $C/12$  to protect the battery from overheating. The minimum current is set to  $C/100$ , corresponding to a battery 100% state of charge, according to Fig. 3. When the battery is fully charged, the PV panel will feed the load directly and the battery charging current is regulated to  $I_{trickle}$  to compensate for the control system power consumption and the battery self-discharge.

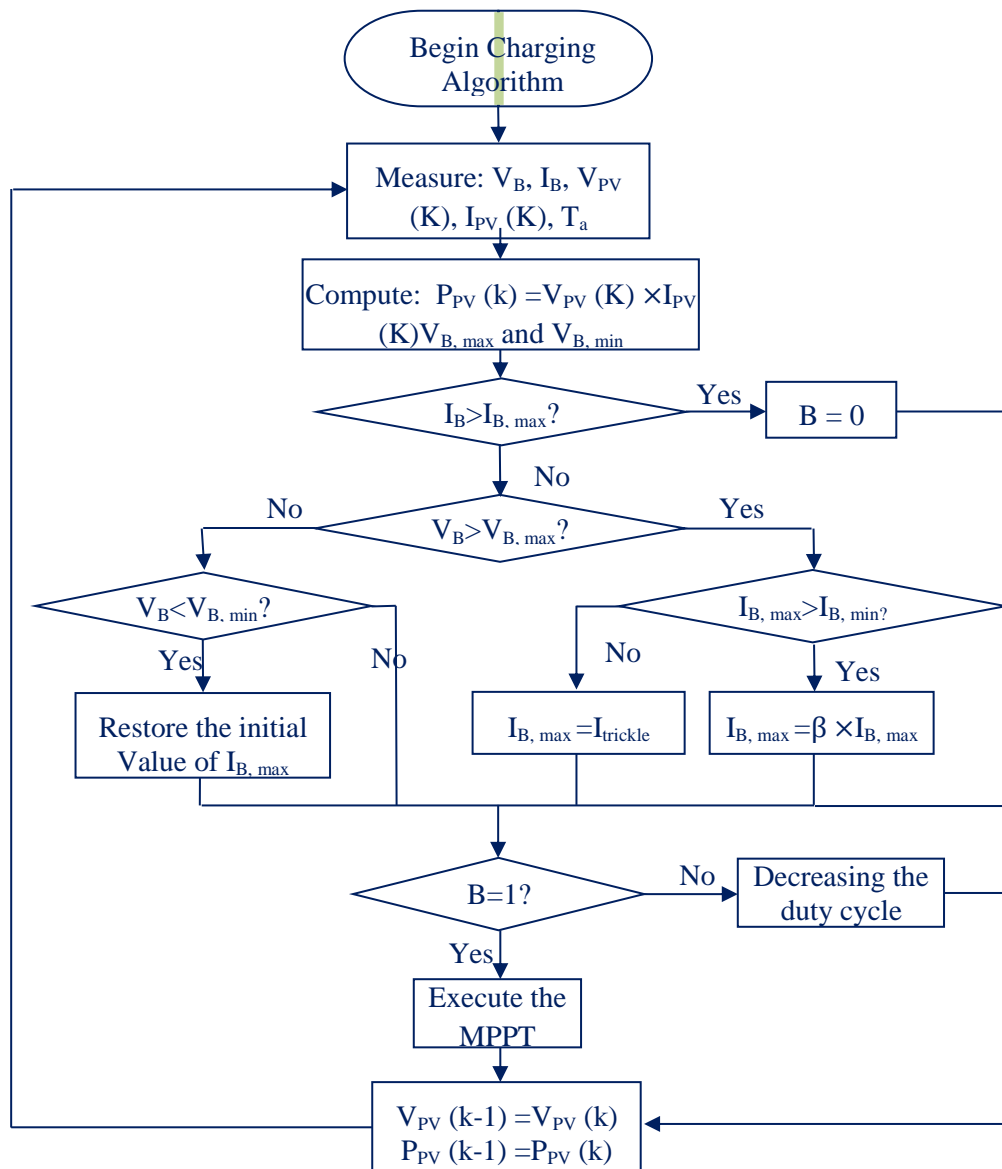


Figure 7. Control algorithm flowchart of a lead-acid battery charging

The minimum and maximum battery voltage levels are then calculated as [3] [4]:

$$V_{bat,max} = 28.8 + (T_a - 25)N_C\alpha \tag{15}$$

$$V_{bat,min} = 25.4 + (T_a - 25)N_C\alpha \tag{16}$$

The initial values of this set of variables are given in Table 2,[4].

Table 2.The Initial Values of the Program Variables [4]

Variable	Initial value
Minimum battery current ( $I_{B, min}$ )	C/100
Maximum battery current ( $I_{B, max}$ )	C/12
Trickle current ( $I_{trickle}$ )	C/100 =2A
Minimum battery voltage ( $V_{B, min}$ )	25V at 25°C
Maximum battery voltage ( $V_{B, max}$ )	28.8V at 25°C
MPPT control action, B	1

Perturbation and observation (P&O) MPPT method is most commonly used among various MPPT algorithms because it is easy to implement. This algorithm is shown in Fig. 8, [9] & [10].

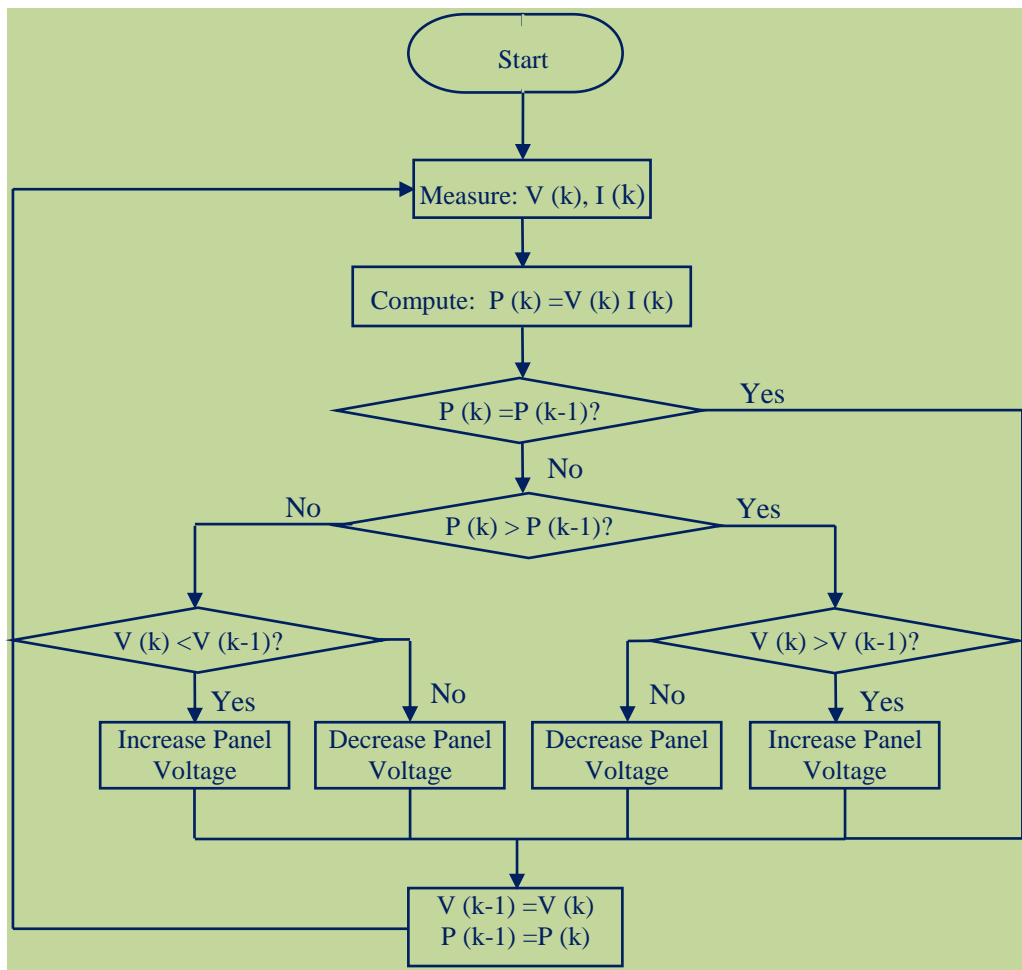


Figure 8.Flowchart of P&O MPPT algorithm [9]

### 6. Results

Table 3 shows the simulation parameter of the PV panel that was used in the simulation program (Proteus).

Table 3.Simulation Parameters of PV Panel

Parameter	Value
Peak Power, PMPP (W)	481
Peak power current, IMPP (A)	15.8
Peak power voltage, VMPP (V)	30.44
Open circuit voltage, VOC (V)	38.2
Short circuit current, ISC (A)	16.4

Fig. 9 presents the PV output current, power versus the output voltage for the variable load for the PV panel that used in this research.



Figure 9. PV output current, power versus the output voltage to a variable load

The simulation curves in Fig. 10 shows the relationship between the cell voltage and the state of charge (SOC) of a lead-acid battery for a fixed ambient temperature  $\theta$  (in these cases,  $\theta = 25^\circ\text{C}$ ), which is built depending on the equations of battery model that is discussed in the section (4.2).

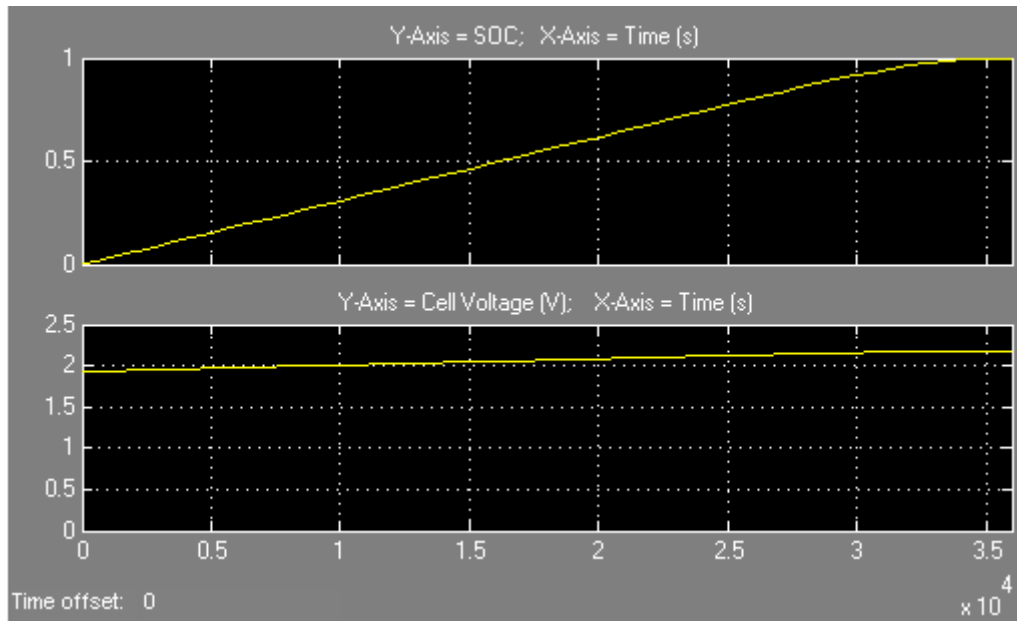


Figure 10. The relation between the cell voltage and the state of charge of the Lead-acid battery

The complete charging process can be divided into three main stages:

First stage is the maximum charging current period, this stage will continue until the battery voltage reaches overcharging limit. Second stage is the period when the current is decreasing from greatest allowed current to the trickle current. The last stage represents the trickle charging current period.

Fig. 11 shows the charging current and voltage at maximum charging stage. PV panel will be runs at maximum power point in this charging stage. Where the output power, current and voltage of the panel are agreement to that in the Table 3.

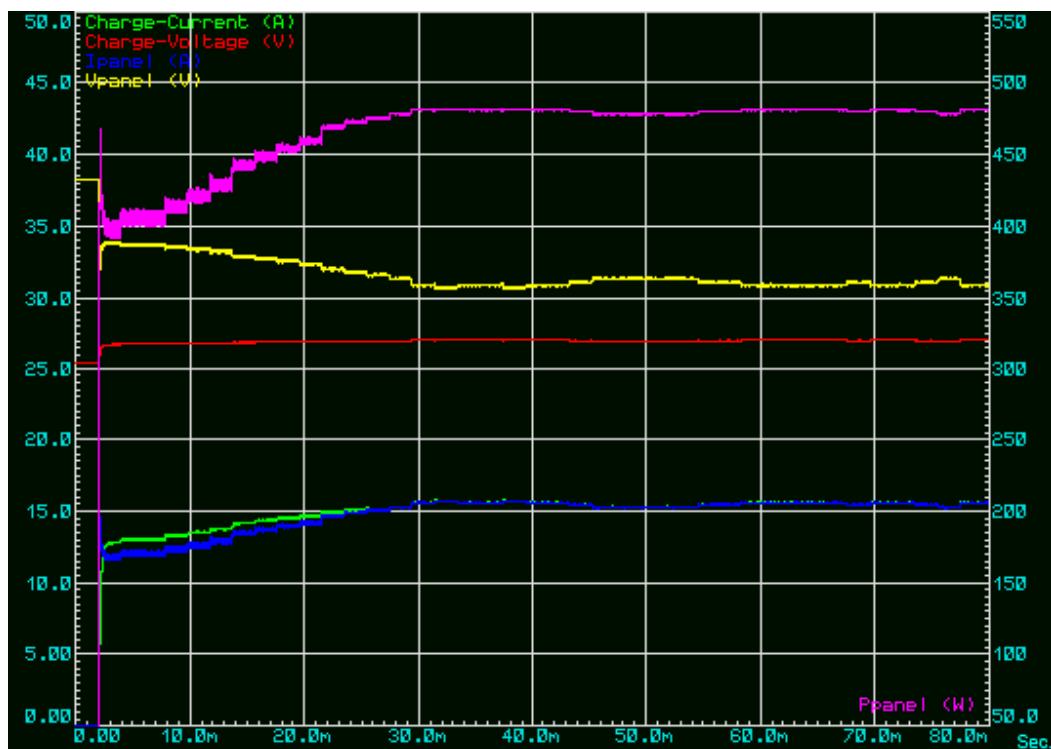
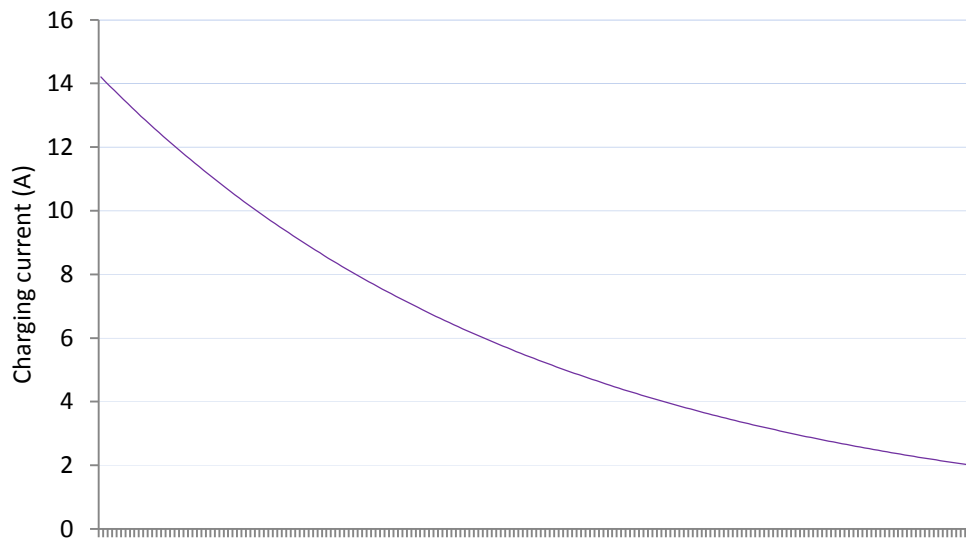


Figure 11. The charging voltage and current at maximum charging stage

Fig. 12 shows the charging current at decreasing charging stage at reduction coefficient ( $\beta$ ) equal 0.99. The current value that noted at each step that gassing voltage is reached programmed as a maximum current value for the next step.



Steps of charging voltage reaches the overcharging limit

Figure 12. The charging current at decreasing charging stage

Fig. 13 shows the charging voltage and current at trickle charging stage. As shown in this figure, the filter inductance will be operates in DCM in this stage of charging.

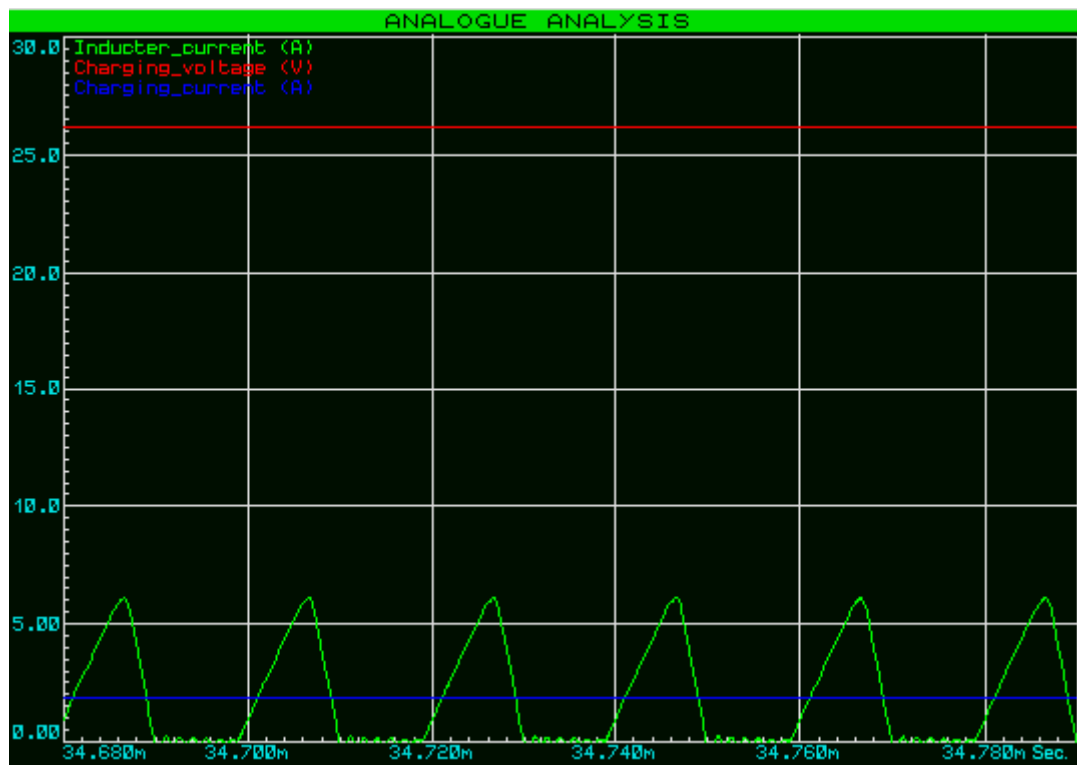


Figure 13. The charging voltage and current at the trickle charging stage

Also, in this proposed system, the following conditions are considered:

- The battery will be feeding the load as long as its voltage is higher than 24V.
- When the battery closes to full charge where the charging current closes to the trickle current (about  $C/50$  i.e. 4A), the power of PV panel can be exploited for other applications.
- The battery separated from the charger and load as long as its terminal voltage is less than the normal value (Less than 22V) or the charging current is less than  $I_{trickle}$ , which foretelling the existence of fault in the battery (short circuit or open circuit of battery cells), so, in this case, an alarm indicator must be used.

These conditions can be happening programmatically by running the relays connected between the battery and charger, the battery and load and the PV panel and other load (any other applications).

Also, in this charger system, there is flexibility for the user by three external switches (S1, S2 and S3). Where through observation the state of charging current that displayed in LCD screen, the user can be adopting the suitable proceeding by externally controlling of system using these switches.

Fig. 14 shows these three external switches (S1, S2 and S3).

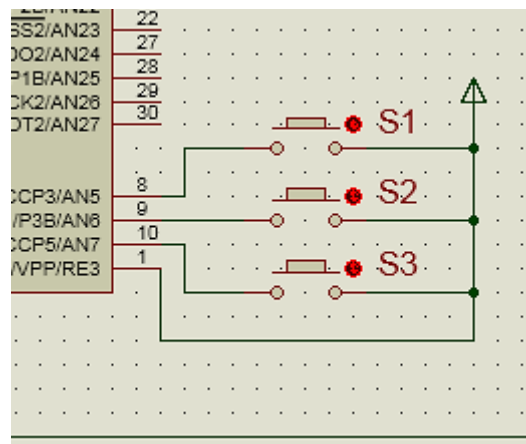


Figure 14. External switches (S1, S2 and S3) for flexibility the proposed system

## 7. Conclusions

This work presents the design of an intelligent charger, avoids the overcharging and gassing problems in Lead-Acid batteries. This charger increases the lifetime of the storage battery, which is the most expensive part of the solar system because it is required to be replaced in a short time as compared with the PV panels.

The flexibility of this charger is very important due to the load requirements and the effect of the ambient natural variations like temperature and irradiation. Also, it takes into consideration the state of charge of the batteries and their faults.

This design can be extended to control the charging process for more number of batteries by design and implement a powerful charger. The information of the state of charge of each battery and to assign whether the battery is "healthy" or "faulty" is required in order to control the charging process by such intelligent charger.

## Symbols

$C_{\min}$	Minimum capacitance of DC-DC converter (F)
$C_{10}$	Battery nominal (rated) charge capacity (Ah)
$C_I$	Battery actual capacity under the actual discharge current I (Ah)
$C_n, C/n$	The charging current at a rate of (battery capacity/ n hours) (A)
D	Duty cycle
$f_c$	Switching frequency (kHz)
$I^*$	Nominal battery current (A)
$I_{LB,max}$	Maximum boundary current of inductance (Average value) (A)
$I_m$	Actual charge main branch current (A)
$I_{O,min}$	Minimum output current to operate in CCM (A)
$K_E$	Temperature coefficient of a lead-acid battery cell (V/°C)
L	Convertor inductance ( $\mu$ H)
$L_{\min}$	Minimum inductance of DC-DC converter ( $\mu$ H)
$Q_e$	Charge consumed from the battery (Ah).
$T_a$	Ambient temperature
$V_S, V_O$	Input and output voltage of Buck Convertor.
$V_{PN}$	Parasitic branch voltage (V)
EMF	Battery cell voltage (V)
$\alpha$	Relative activity of the electrolyte (V/°C/cell)
$\beta$	Reduction coefficient
$\Delta V_O$	Ripple of the output voltage of Buck convertor (V)
$\theta$	Electrolyte temperature (°C)
$\theta_f$	Electrolyte freezing temperature (-40°C)
$\tau$	Time constant of the main branch (s)
$N_C$	Number of cells of the battery stack ( $N_C = 12$ )

## Abbreviations

SOC	State of charge
DOC	Depth of charge
SOH	State of health
SG	Specific Gravity (kg/L)

## 8. References

1. David Linden and Thomas B. Reddy, (1995). "*Handbook of Batteries*". 3<sup>th</sup> ed., ISBN 0-07 -135978-8, Printed in the United States of America.
2. Shen Guo, (2010). "*The Application of Genetic Algorithms to Parameter Estimation in Lead-Acid Battery Equivalent Circuit Models*", A Thesis Presented to the University of Birmingham.
3. Ola Subhi Waheed Al-Qasem, (2012). "*Modeling and Simulation of Lead- Acid Storage Batteries within Photovoltaic Power Systems*", A Thesis Presented to the An-Najah National University, Palestine.
4. E. Koutroulis and K. Kalaitzakis, (2004). "*Novel Battery Charging Regulation System for Photovoltaic Applications*", IEE, Technical University of Crete, Chania, Vol. 151, No. 2, P.P. 191-197.

5. Tiezhou Wu, Qing Xiao, Linzhang Wu, Jie Zhang and Mingyue Wang, (2011) "*Study and Implementation on Batteries Charging Method of Micro-Grid Photovoltaic Systems*", Smart Grid and Renewable Energy, P.P. 324-329.
6. Ned Mohan, William P. Robbins, University of Minnesota, Minnesota, Tore M. Undeland, (2003). "*Power Electronic Converters, Applications, and Design*", Norwegian University of Science and Technology, Norway Third Edition, USA ISBN 978-0-471-22693-2 WIE ISBN 0-47 1-42908.
7. Massimo Ceraolo, (2000). "*New Dynamical Models of Lead–Acid Batteries*" IEEE Transactions on Power Systems, Vol. 15, p.p.1184 -1190, November.
8. Nazih Moubayed, Janine Kouta, Lebanese University – Lebanon, Ali EI-Ali, Hala Dernayka and Rachid Outbib, Aix-Marseille III University, Marseille – France, "*Parameter Identification of the Lead-Acid Battery Model*", IEEE, 2008.
9. Sree Manju, Ramaprabha and Mathur, "*Design and Modeling of Standalone Solar Photovoltaic Charging System*", (2011). Department of EEE, SSN College of Engineering, Vol. 18– No.2, p.p. 41-45.
10. Mei Shan Ngan and Chee Wei Tan, (2011). "*A Study of Maximum Power Point Tracking Algorithms for Stand-alone Photovoltaic Systems*", IEEE, University Teknologi Malaysia, Malaysia, p.p. 22-27.